

University of Groningen

## Strain and composition effects in epitaxial ferroelectrics

Rispens, Gijsbert

**IMPORTANT NOTE: You are advised to consult the publisher's version (publisher's PDF) if you wish to cite from it. Please check the document version below.**

*Document Version*

Publisher's PDF, also known as Version of record

*Publication date:*

2010

[Link to publication in University of Groningen/UMCG research database](#)

*Citation for published version (APA):*

Rispens, G. (2010). *Strain and composition effects in epitaxial ferroelectrics: structural studies on  $Pb_xSr_{1-x}TiO_3$  thin films grown by MBE.* s.n.

### Copyright

Other than for strictly personal use, it is not permitted to download or to forward/distribute the text or part of it without the consent of the author(s) and/or copyright holder(s), unless the work is under an open content license (like Creative Commons).

The publication may also be distributed here under the terms of Article 25fa of the Dutch Copyright Act, indicated by the "Taverne" license. More information can be found on the University of Groningen website: <https://www.rug.nl/library/open-access/self-archiving-pure/taverne-amendment>.

### Take-down policy

If you believe that this document breaches copyright please contact us providing details, and we will remove access to the work immediately and investigate your claim.

Downloaded from the University of Groningen/UMCG research database (Pure): <http://www.rug.nl/research/portal>. For technical reasons the number of authors shown on this cover page is limited to 10 maximum.

## Chapter 2

# Growth of $\text{Pb}_x\text{Sr}_{1-x}\text{TiO}_3$ thin films using MBE

### 2.1 Introduction

The growth of  $\text{PbTiO}_3$  films has been reported using various methods such as sputtering [53], pulsed laser deposition [54], sol-gel methods [55] and MOCVD [56, 57]. The growth of  $\text{PbTiO}_3$  using Molecular Beam Epitaxy (MBE) methods has been reported only by a few groups. [58–60] The main issues in the growth of  $\text{PbTiO}_3$  thin films using MBE are the oxidation of Pb and the stoichiometry. Despite the difficulties of growing  $\text{PbTiO}_3$  using MBE, as indicated by the low number of literature reports, the nature of the MBE process promises a very high level of control and reproducibility.

In this chapter, the MBE growth process, as well as Reflection High Energy Electron Diffraction (RHEED) technique, which is an *in-situ* probe of the growth process, will be explained. The details of the adsorption controlled MBE growth of  $\text{PbTiO}_3$  and  $\text{Pb}_x\text{Sr}_{1-x}\text{TiO}_3$  on various substrates will be shown in second half of the chapter.

## 2.2 Molecular Beam Epitaxy

Molecular Beam Epitaxy is a growth technique in which the reactants arrive at a heated substrate surface in the form of molecular or atomic beams. The molecular beams are formed by evaporation of the reactants into (ultra) high vacuum. In a typical MBE experiment, Reflection High Energy Electron Diffraction (RHEED) is used for in situ control.

Figure 2.1 shows a schematic representation of a typical MBE setup for the growth of oxides. The beam sources are mounted in a vacuum chamber pointing toward the sample. For solids, various types of evaporation sources can be used, such as effusion cells and e-beam evaporators. For oxidation of the films, oxidizing gas is supplied through a tube. The material beams can be covered by shutters for precise control over the growth. RHEED is used not only to give valuable information on the growing surface, but also to provide feedback for the control of the shutters. Electrons with energies between 10 and 30 KeV are provided by an electron gun, reaching the sample under a small angle (1 to 3°) to ensure surface sensitivity. The diffracted electrons are made visible by a fluorescent screen.

The molecular beams can be created by various types of sources. The effusion or Knudsen cell is a very common type of source. In an effusion cell the material is evaporated from a crucible that is surrounded by a heating coil. Depending on the properties of the source material evaporation takes place either from the solid phase or from the melt. Most often alumina crucibles are used, but if necessary various (metal) liners can be used to prevent unwanted effects such a diffusion through the alumina or oxidation of the source.

For materials that require a (very) high temperature for evaporation, such as titanium, electron beam (e-beam) evaporators can be used. In this case heating is achieved through bombardment with electrons. We have used the Focus EVF evaporator for e-beam heating. In this type of evaporator electrons are emitted from a circular filament that is positioned slightly above either a rod or a crucible with evaporant. A high voltage is applied between the evaporant and the filament, accelerating the electrons towards the evaporant. For rod evaporation this requires

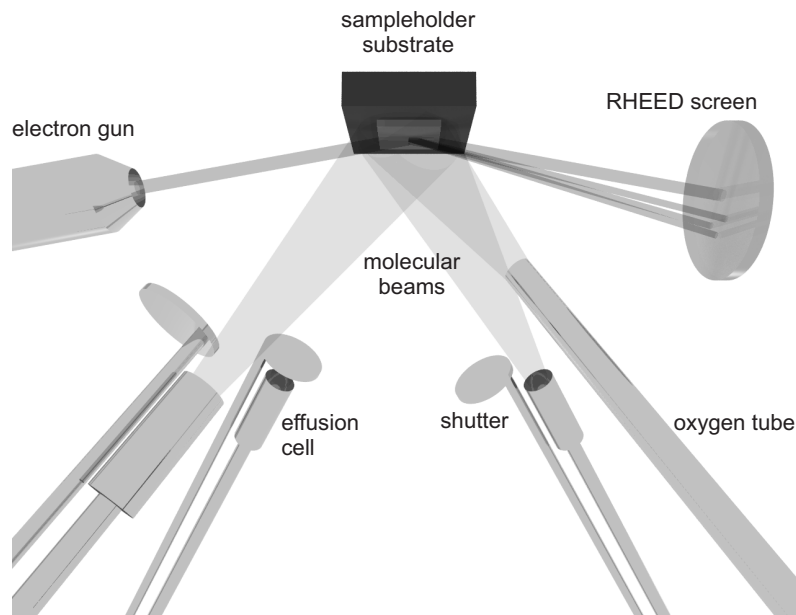


**Figure 2.1:** Schematic drawing of the inside of a MBE chamber.

the melting point to be above the evaporation temperature.

Oxidizing gas is supplied through a tube connected to a leak valve. The tube ends close to the substrate, increasing the oxidizing gas pressure at the substrate. Molecular oxygen can be used as an oxidizing gas, but to increase the oxidizing power  $O_3$  [60],  $NO_2$  [61],  $H_2O_2$  [58] or oxygen plasma (atomic oxygen,  $O\cdot$ ) [62] can be used as alternatives.

MBE growth experiments can be conducted in various ways. The most common way is co-evaporation, where two or more beams are arriving simultaneously at the substrate. This requires exact matching of the flux of the impinging beams. For more complex materials, modulated beam techniques may be used. In modulated beam MBE, the beams are shuttered to obtain the desired stoichiometry. Using this technique, the deposition of materials is achieved by depositing sublayers of less complex materials. This is often used for the growth of perovskite oxides ( $ABO_3$ ), that consist of stacked AO and  $BO_2$  simple oxide layers.

### 2.2.1 Vacuum requirements for MBE

The beam nature of the particles impinging on the substrate surface is one of the characteristic features of the MBE process. For the growth of sharp interfaces a beam of material can be controlled by a shutter. Shuttering of the beams can also be used to control the stoichiometry or doping levels in a film. In the case of evaporation of a material into ambient pressure or low vacuum, a cloud of material is formed through collisions. Such a cloud cannot be controlled with similar precision as the particles would have a random direction and velocity giving rise to a spread in arrival times. Growth from beams also changes the kinetics with respects to normal evaporation. In the case of condensation of particles from a cloud, the average kinetic energy of the particles will be determined by the temperature of the background gas. The particles coming from a beam have not undergone collisions and so the kinetic energy or temperature of the particles is determined by the evaporation temperature.

Ensuring the formation of molecular beams sets the upper limit for the background pressure during the MBE process. The mean free path of the particles should be larger than the distance between the source and the sample. This upper value depends on the material evaporated and the background gas. The maximum pressure for beam formation is [63]

$$p = k_B T \frac{L^{-1} - \sqrt{2}\pi n_b d_b^2}{\pi d_{bg}^2} \quad (2.1)$$

with

$$d_{bg} = \frac{d_b + d_g}{2}$$

Where  $L$  is the distance between the outlet of the source to the substrate,  $k_B$  is the Boltzmann constant,  $T$  is the background temperature,  $n_b$  is the concentration of particles in the beam,  $d_b$  and  $d_g$  are the diameter of the beam particles and the background gas particles, respectively. Typical data for the PbO beam used in MBE growth of  $\text{PbTiO}_3$  are:

$$T = 298\text{K}, L = 40\text{cm}, d_b = 4.24\text{\AA}, d_g = 1.32\text{\AA}, n_b = 1.03 \times 10^{15}\text{m}^{-3}$$

For these values, equation 2.1 gives a maximum admissible pressure for beam formation of about  $4 \times 10^{-5}$  mbar. This is higher than the oxygen background pressure of  $5 \times 10^{-6}$  mbar used during growth of  $\text{PbTiO}_3$  and thus  $\text{PbO}$  evaporates into molecular beams. For the other source materials used in the growth of  $\text{Pb}_x\text{Sr}_{1-x}\text{TiO}_3$  thin films, the maximum admissible background pressures are even higher.

The amount of particles from the residual gas that impinge on the substrate surface is given by [63]

$$f_i = p_i \sqrt{\frac{N_A}{2\pi k_B M_i T_S}} \quad (2.2)$$

where  $p_i$  is the partial pressure,  $N_A$  is the Avogadro constant,  $M_i$  is the molecular mass and  $T_S$  is the substrate temperature. For our MBE system, the residual gas pressure is around  $2 \times 10^{-8}$  mbar at the growth conditions. If we assume that the residual gas consists mainly of  $\text{N}_2$  ( $M_i = 28.02$  g/mol), equation 2.2 then gives, for a substrate temperature of  $600^\circ\text{C}$ , an impingement rate of  $6.7 \times 10^{16}$  atoms  $\text{m}^{-2}\text{s}^{-1}$ . This value is comparable to the number of particles arriving from the molecular beams, which is around  $1 \times 10^{17}$  atoms  $\text{m}^{-2}\text{s}^{-1}$ , so the number of impurity atoms arriving at the substrate surface every second is close to the number of atoms from the molecular beams. However, as most of the impurity species are fairly inert, their sticking coefficient is quite low, which largely limits the incorporation of impurities. A low sticking coefficient for the residual gas particles on the heated substrate surface is more important for the growth of clean films than the low residual gas pressure.

### 2.2.2 Growth processes in thin film growth

The growth of thin films takes place at the substrate or film surface. Figure 2.2 shows the basic processes that can take place at the surface. Particles arrive at the sample surface and can then diffuse over the surface until they are either incorporated into the crystal or re-evaporates. The ratio between the particles incorporated into the lattice and the total number of particles is called the sticking coefficient.

Incorporation into the crystal can take place in various ways. A particle can be

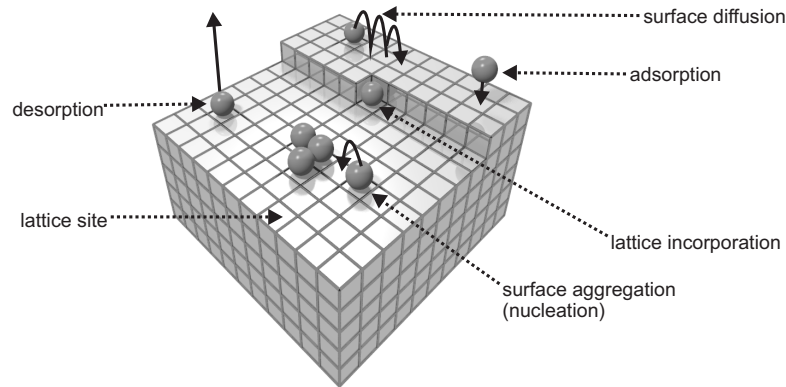


**Figure 2.2:** Schematic illustration of the surface processes that take place during epitaxial growth [64, 65]

incorporated at special sites such as a surface steps, dislocations or defects. The density of such special sites is an important parameter in growth. Particles can also aggregate to form clusters. At small sizes, these clusters are not stable against dissociation and re-evaporation. If a cluster is larger than a critical size, the cluster can act as a nucleus for crystal growth. [64–66] The size of these critical nuclei depends on the change in chemical potential upon forming the cluster and the surface energy of the cluster.

If the temperature is low, the critical nucleus size can be as small as a few atoms

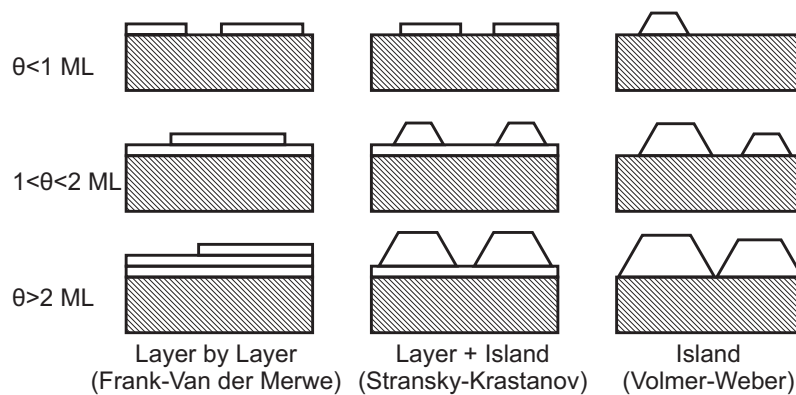


**Figure 2.3:** Representation of the basic growth modes in thin film growth.  $\theta$  is the mono-layer coverage [64]

and the density of nuclei will be large. In this case growth takes place through coalescence of clusters. This can result in a grainy structure. At high temperatures the critical nucleus size is large resulting in growth from a small number of clusters and/or growth from special sites. In the step-flow growth mechanism, for instance, growth takes place exclusively at crystal steps. Figure 2.3 shows the three basic growth modes observed in thin film growth [64]. For all these modes perfect surfaces are assumed and thus growth from special sites is not taken into account.

Layer-by-layer or Frank-Van der Merwe growth, is a growth mode by which each layer is filled before the next layer nucleates. For this growth mode to occur the surface energy of the growing film should be low enough to prevent formation of 3D clusters. Furthermore, the density of particles in a new layer should be low enough to prevent the formation of critical nuclei as long as the growing layer is not complete. For this, the size of the critical nucleus should be large and thus the temperature should be high enough. The combination of a small density of critical nuclei and completion of a layer before nucleation of the next makes that layer-by-layer growth results in smooth films and sharp interfaces.

In island or Volmer-Weber growth, islands, rather than completely filled layers are formed. This growth mode occurs when the total surface energy of the film is higher than that of the substrate. Island formation minimizes the energy in this case. Island growth results in rough films, which is generally not preferred. However, if the islands nucleate in predetermined, regular sites, island growth can be used for the formation of structures such as quantum dots.

The intermediate between layer-by-layer and island growth is layer-plus-island growth or Stransky-Krastanov growth. Here, after one or a few monolayers the growth mode changes from layer-by-layer to island growth. In this case the total surface energy of the growing film switches from being smaller to being larger than that of the substrate. This can occur if the interfacial energy changes as the film grows.

The classification of growth modes discussed above is based on thermodynamics. Accordingly, when deciding the growth conditions, the substrate temperature is the main parameter to change the growth mode. However, the kinetics play an



equally important role in the control of thin film growth. A too low temperature in layer-by-layer growth, for instance, can cause the growth of island due to a too short diffusion length or a too high number of critical nuclei.

In conclusion, epitaxial growth is governed by both kinetics and thermodynamics. Growth from special sites, especially substrate steps, is something that also has to be taken into account when discussing epitaxial growth.

### 2.3 Reflection High Energy Electron Diffraction

Reflection High Energy Electron Diffraction (RHEED) is a surface sensitive electron diffraction technique that can be used *in-situ* during growth. The RHEED setup consists of a electron gun emitting electrons with an energy between 10 and 30 keV. This electron beam reaches the surface of the growing film at an angle of about  $3^\circ$ . The diffracted electron beams are imaged on a fluorescent screen. The image is recorded using a CCD camera.

RHEED can give information about the surface structure and morphology during growth. Variations in the diffracted pattern can also be used to identify impurities or unwanted phase. In layer-by-layer growth, oscillations in the diffracted intensity give information about the growth rate and allows the growth to be controlled with atomic precision.

RHEED is a surface sensitive technique since both the incident angle and the probing angle are small. Moreover, the interaction between electrons and matter is strong and thus the mean free path quite small [67]. The magnitude of the electron momentum is determined by the kinetic energy,  $E$ .

$$k_0 = \frac{1}{\hbar} \sqrt{2m_0E + \frac{E^2}{c^2}} \quad (2.3)$$

where  $m_0$  is the rest mass of the electron. The second term under the square root is the relativistic contribution, which amounts to about 3% for 20 keV electrons.

Figure 2.4 shows both the real space geometry of the RHEED experiment and the Ewald sphere construction for finding the diffraction conditions. Diffraction

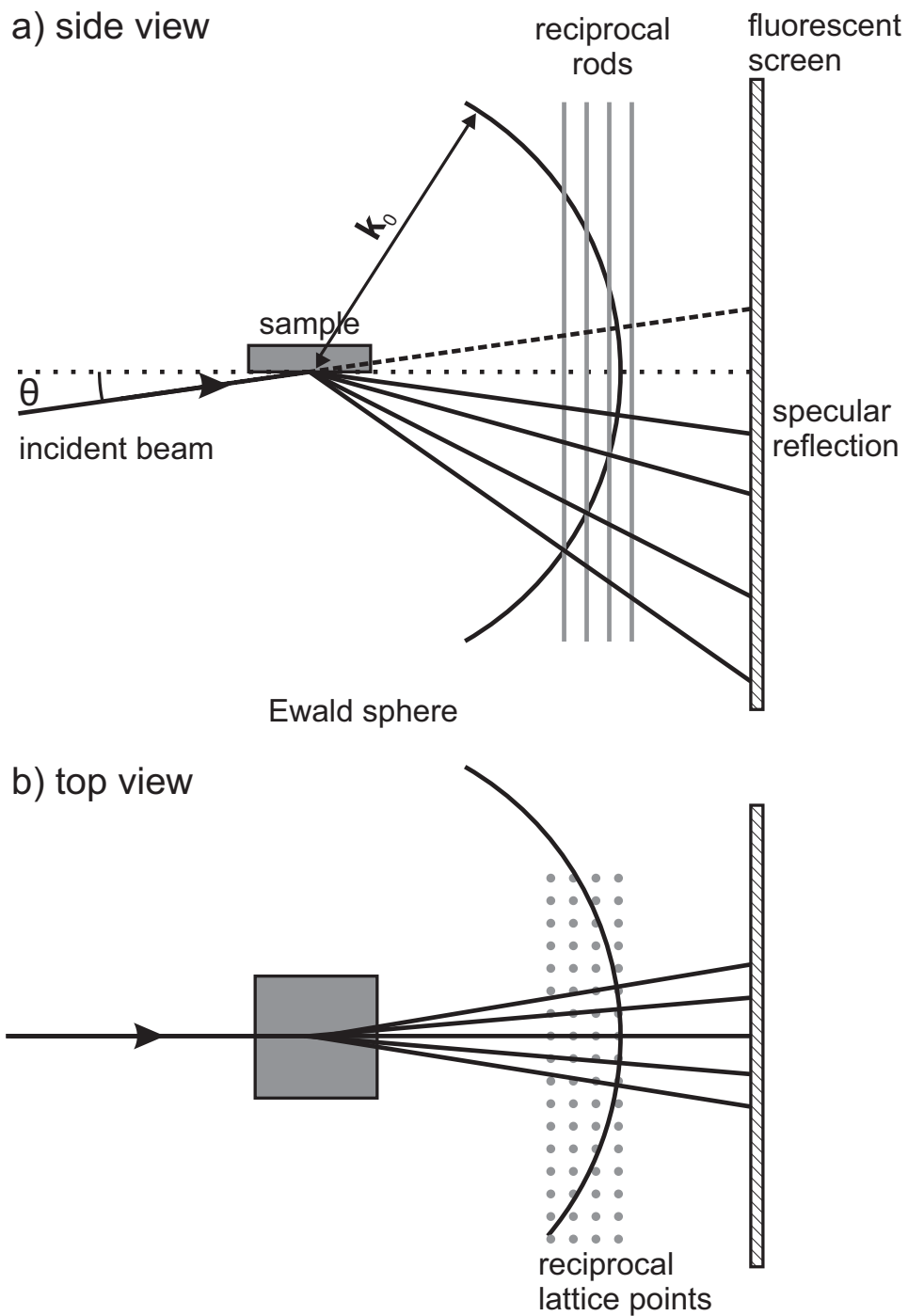


**Figure 2.4:** Ewald's sphere construction and diffraction geometry of RHEED. a) side view. The intersections of the Ewald's sphere with the reciprocal space rods are the positions where the diffraction conditions are fulfilled. b) Top view.

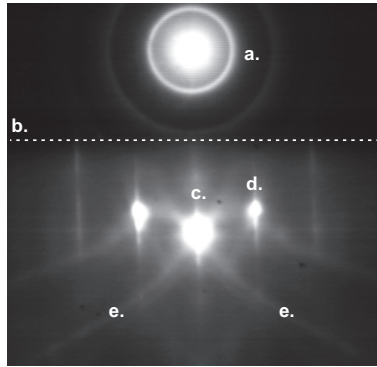


**Figure 2.5:** RHEED pattern of a  $\text{SrTiO}_3$  substrate. a) direct beam. b) shadow edge, c) specular (00) spot. d) off-specular (01) spot. e) Kikuchi lines

experiments probe reciprocal space (see section 3.2.1). Since RHEED is only sensitive to the surface, the electrons see no periodic lattice in the out-of-plane direction and thus, the reciprocal lattice points form rods in that direction. In the in-plane directions there is periodicity and the reciprocal lattice consists of points.

In the ideal case of a perfectly flat crystal and no divergence of the electron beam, the RHEED pattern would consist of spots on a circle. In a real experiment, however, beam divergence and crystal steps can cause some spread in  $k_0$ , and thus the radius of the Ewald's sphere. As the diffraction condition is less strict in the out-of-plane direction, the spots can elongate in this direction to form streaks. Figure 2.5 shows the RHEED pattern of a  $\text{SrTiO}_3$  substrate. Three diffraction spots are clearly visible, the specular, or 00, spot and two off-specular, 01 and  $0\bar{1}$ , spots. The interaction between electrons and matter is strong and thus inelastic scattering and multiple scattering effects also take place. Kikuchi lines (fig. 2.5 e) are one of the features that arise due to multiple scattering. Kikuchi lines can be explained by a two step model. In the first step the direction of the incident beam is randomized by collisions. In these collisions the energy loss should be small. In the second step, the isotropic radiation resulting from the first step diffracts by the lattice. [68].

In island growth, the transmission of the electrons through the growing islands can occur. As the diffraction geometry is different in this case, the pattern changes dramatically. Figure 2.6 shows a typical 3D transmission pattern of PbO islands on  $\text{SrTiO}_3$ . Various intermediate cases between a pure reflection pattern (fig.2.5) and a

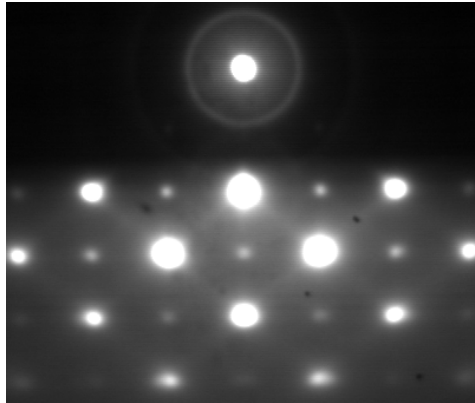


**Figure 2.6:** 3D transmission pattern of PbO islands on SrTiO<sub>3</sub>

pure transmission pattern (fig. 2.6) can occur depending on the size and spacing of the islands. As the diffraction conditions for both cases are completely different, it is possible to distinguish reflection and transmission contributions by rotating the azimuth of the sample. Reflection spots will move, whereas transmission spots will not.

As RHEED is only sensitive to the surface, monitoring the RHEED pattern during growth gives information about the growing layer and the formation of secondary phases and surface reconstructions. [69] In some cases it is possible to adjust the growth conditions to remove or minimize unwanted phases.

### 2.3.1 RHEED Oscillations

During layer-by-layer growth, the intensity of the RHEED spots oscillates as a function of layer coverage. The oscillation period then corresponds to exactly one monolayer. RHEED oscillations give real-time feedback on the growth process and can be used to determine growth rates. Growth of multilayers benefits from RHEED oscillations as sharp interfaces can be attained by stopping growth of one of the multilayer components at a RHEED maximum. RHEED oscillations are probably the main reason why the use of RHEED is so widely spread in epitaxial growth.

There are various models trying to describe RHEED oscillations. [68] A periodic variation of the surface roughness during growth is one of the most common

explanations. This model states that nucleation on a smooth surface increases the roughness and thus decreases the reflectivity of the surface and the intensity of the spots. The roughness reaches a maximum at a coverage of exactly 50% and then decreases until the nucleated layer is completely filled. This model relates the oscillations to the layer coverage through the density of steps creating roughness.

A second, diffraction based, model is based on the existence of (destructive) interference between electrons scattered from the growing layer and the filled layers below. In this case, the amount of destructive interference depends directly on the coverage of the growing layer. But, although this model can reproduce intensity oscillations, in kinetic theory no oscillations are predicted exactly at the Bragg condition. At the Bragg position the interference between both layers is constructive by definition.

An important discrepancy between both models and experiment is that they cannot account for the phase shifts that are often observed between specular and off-specular peaks, which are a function of the incident angle. [70] These phase shifts suggest that there is no simple relationship between the RHEED oscillations and the coverage or step density. Dynamical scattering theory is required to model these observations. However, as dynamical scattering theory of static events is already quite involved, accurate modeling of a dynamic process such as crystal growth is very difficult. [68] Various experimental results on RHEED oscillations show a dependence on either step density or coverage and theoretical modeling cannot explain all observations based on either origin alone. The conclusion at the moment seems to be that no single electron scattering or interference process is able to account for all experimental observations. [71]

Most work on RHEED oscillations has been done on GaAs and related semiconductor systems grown in co-evaporation. For the growth of complex oxides using MBE it is common to use shuttered beams. [69, 72, 73] This complicates the analysis of RHEED intensity variations. The elements of different sublayers can have very different scattering strengths, which can result in periodic intensity variations driven by shuttering. The surface structure can also be different for the different sublayers, giving a periodic variation of the RHEED pattern. Within the growing

sublayer, layer-by-layer growth driven oscillations may be observed.

Models for layer-by-layer growth driven oscillations are still not fully developed. However, the relation between the period and monolayer growth is well established, and as a result most discussion about RHEED oscillations is empirical in origin, especially in the case of modulated beam growth of complex oxides where various other factors influence the RHEED intensity.

## 2.4 Substrates

### 2.4.1 Strontium Titanate

Strontium titanate ( $\text{SrTiO}_3$ ) is the substrate material that has been used for most films described in this thesis.  $\text{SrTiO}_3$  is a cubic perovskite material and is structurally compatible with  $\text{PbTiO}_3$ . At room temperature it has a lattice parameter of 3.905 Å [74], which is a very good lattice match with the short axis of tetragonal  $\text{PbTiO}_3$ . [60, 75]  $\text{SrTiO}_3$  substrates are widely used for the growth of oxide thin films.  $\text{SrTiO}_3$  substrates obtained from various suppliers have been used. Most substrates were obtained from either CrysTec GmbH or SurfaceNet GmbH.

Along the [001] direction the  $\text{SrTiO}_3$  consists of alternating SrO and  $\text{TiO}_2$  layers. The surface of cleaved and polished  $\text{SrTiO}_3$  (001) substrate consists of terraces with both  $\text{TiO}_2$  and SrO termination. These terraces are separated by half a unit cell. For reproducible growth and sharp interfaces single terminated substrates are required. It is possible to obtain  $\text{SrTiO}_3$  substrates with a single termination by a chemical treatment with a HF/ $\text{NH}_4\text{F}$  buffer solution. [76] We have used the treatment as described by Koster et al. [77]

As-received substrates are cleaned with both acetone and ethanol using an ultrasonic bath. The substrates are dried by blowing nitrogen. The next step is a reaction with ultra pure (18M $\Omega$ ) water in an ultrasonic bath. The basic SrO on the substrate surface reacts with water to form  $\text{Sr}(\text{OH})_2$ . The surface  $\text{Sr}(\text{OH})_2$  is removed by reaction with a HF/ $\text{NH}_4\text{F}$  buffer solution with a pH of 4.5. This reaction takes place under ultrasound for 30 seconds. After the reaction the substrates are quickly rinsed with water three times. Rinsing with ethanol and drying using

Miscut	Time
$0.06^\circ$	2h
$0.1^\circ$	1h30min
$0.2^\circ$	1h

**Table 2.1:** Timing used for heat treatment at  $960^\circ\text{C}$  of  $\text{SrTiO}_3$  substrates of different miscuts

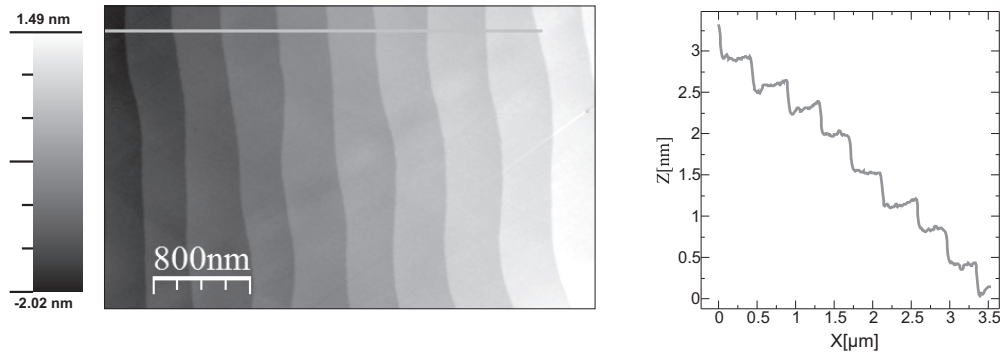


**Figure 2.7:** Tapping mode AFM image of a treated  $\text{SrTiO}_3$  substrate. The profile clearly shows a step size of  $\approx 3.9 \text{ \AA}$

nitrogen concludes the chemical treatment.

After chemical treatment, a heat treatment is used to straighten the step edges. The substrates are heated up to  $960^\circ\text{C}$  in a tube furnace under an oxygen flow of  $200\text{cc}/\text{min}$ . The time the substrates are kept at  $960^\circ\text{C}$  depends on the miscut. At higher miscut the distance that particles need to diffuse to be incorporated in a step edge is smaller, and thus, a shorter time is required. The time required for various miscuts can be found in table 2.1.

Figure 2.7 shows an AFM image of a treated  $\text{SrTiO}_3$  substrate. It can be seen that the steps are straight. The line profile across a number of steps shows that the terraces are flat and that the step height is around  $3.9 \text{ \AA}$ . This indicates that the substrate has a single termination.

#### 2.4.2 Dysprosium Scandate

Strontium titanate has been used as a substrate material for many years. More recently, the rare earth scandates have been introduced as substrate materials. The

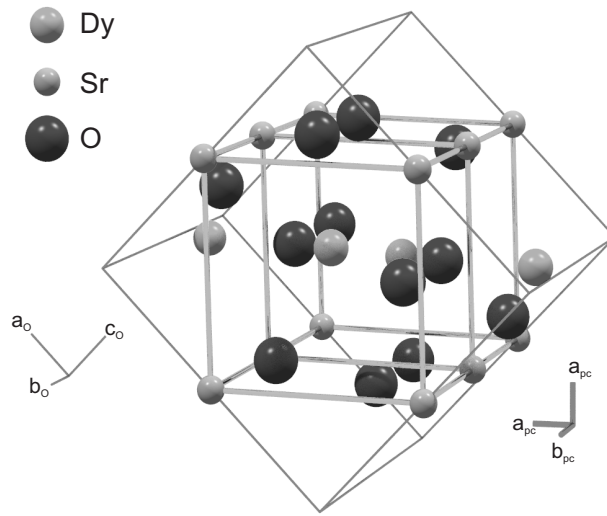


**Figure 2.8:** Structure of  $DyScO_3$ . The edges of both the orthorhombic and pseudo-cubic unit cell are shown.

rare earth scandates have pseudo-cubic lattice parameters ranging from 3.93 Å for  $HoScO_3$  to 4.05 Å for  $LaScO_3$ . The rare earth scandates have an orthorhombic crystal structure, with space group #62 ( $Pnma$ ). [78, 79]

$DyScO_3$  is the scandate that has been used in this thesis for the growth of  $PbTiO_3$  and  $Pb_xSr_{1-x}TiO_3$  thin films. The (110) plane of  $DyScO_3$  has a nearly square lattice. The orthorhombic  $a_O$ ,  $b_O$  and  $c_O$  lattice parameters of  $DyScO_3$  at room temperature are 5.720 Å, 7.890 Å and 5.442 Å respectively. [78, 79] The structure of  $DyScO_3$ , showing both the orthorhombic and pseudocubic cell edges can be found in figure 2.8. The pseudocubic unit cell is obtained by rotating the orthorhombic cell through  $45^\circ$  around the  $b_O$  direction and taking the half of  $b_O$ .

$$a_{pc} = \frac{1}{2}\sqrt{a_O^2 + c_O^2}; \quad b_{pc} = \frac{b_O}{2} \quad (2.4)$$

At room temperature the pseudocubic lattice parameters obtained are  $a_{pc} = 3.947$  Å and  $b_{pc} = 3.945$  Å. These are the in-plane lattice parameters for the (110) orientation.

Along the [110] direction  $DyScO_3$  has a similar AO/ $BO_2$  stacking to  $SrTiO_3$  and



thus a polished surface will have a mixed termination. In contrast to  $\text{SrTiO}_3$  however, no well established surface treatment is available in literature. Karimoto describes a heat treatment at  $1100^\circ\text{C}$  for 12 hours under oxygen flow, followed by etching with 0.1%  $\text{HNO}_3$  in ethanol. [80]. For the substrates used in this thesis the best results were obtained by cleaning with acetone and ethanol followed by a heat treatment at  $1020^\circ\text{C}$ . This results in straight steps with a step height close to  $4\text{ \AA}$ . Keeping the substrates away from any water is very important for getting a good result. Recently, a treatment was found at the University of Twente that results in a single termination as observed from  $\text{SrRuO}_3$  growth. [81] In this procedure, a chemical etching step of 1 hour with a 12M  $\text{NaOH}$  solution in an ultrasonic bath follows the heat treatment. The strong base is then washed off with an 1M  $\text{NaOH}$  solution.

$\text{SrTiO}_3$  consists of uncharged  $\text{TiO}_2$  and  $\text{SrO}$  sublayers, whereas  $\text{DyScO}_3$  consists of  $\text{DyO}_2^-$  and  $\text{ScO}^+$  layers. Thus, a single termination of  $\text{DyScO}_3$  will lead to a charged surface. Which has to be compensated in some way. Most likely compensation mechanisms are either a surface reconstruction or the formation of an adsorbate layer. We have tried to perform LEED studies to look at the surface structure of  $\text{DyScO}_3$  substrates. It was impossible to obtain patterns in both as-received and heat treated substrates. A big improvement in the RHEED pattern is observed when heating from room temperature to the growth temperature. These observations may suggest compensation of the charges by adsorbates.

## 2.5 Adsorption controlled growth of $\text{PbTiO}_3$ using MBE

Stoichiometry is a key issue for MBE growth of  $\text{PbTiO}_3$  and  $\text{Pb}_x\text{Sr}_{1-x}\text{TiO}_3$  thin films. Lead and oxygen deficiencies are most common in  $\text{PbTiO}_3$ . [60, 82, 83] Lead vacancies often coexist with oxygen vacancies to maintain charge neutrality.  $\text{PbTiO}_3$  is not sensitive to oxidation as titanium is in its highest oxidation state and higher oxidation state lead oxides, such as  $\text{Pb}_3\text{O}_4$  and  $\text{PbO}_2$  are not stable at the growth temperature under oxygen pressures lower than ambient. [84] A large overpressure

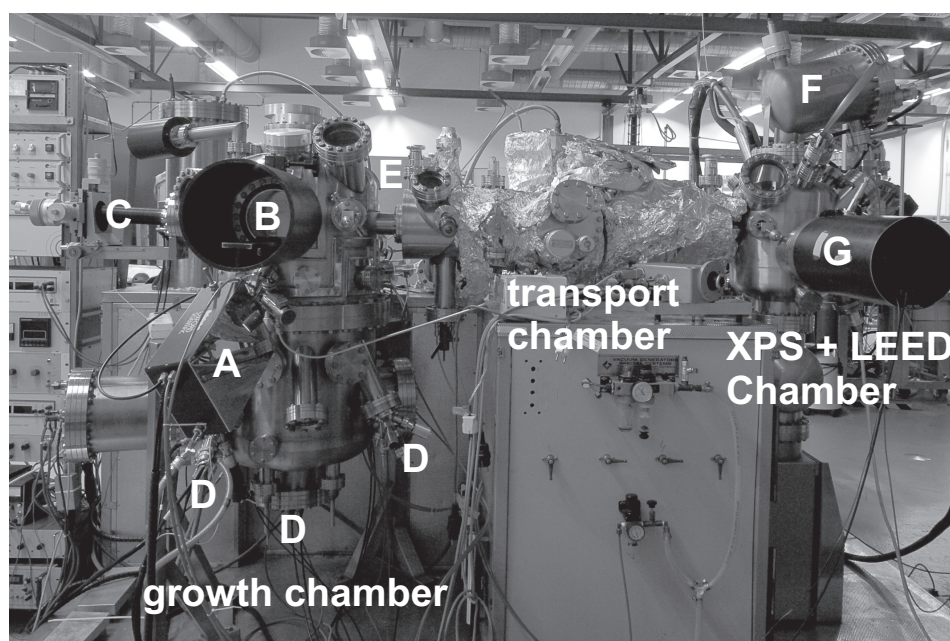


**Figure 2.9:** Picture of the MBE system. a) plasma source b) RHEED screen c) manipulator d) evaporation sources e) load lock (not visible) f) XPS analyzer g) LEED

of oxygen and a RF generated oxygen plasma can be used to prevent oxygen vacancies. For lead vacancies, however, the situation is more difficult as the evaporation temperature for both lead and lead oxide are relatively low, at around  $600^\circ\text{C}$ . [85] Growth takes place at roughly the same temperature and thus, ensuring a proper lead stoichiometry is the main challenge in MBE growth of  $\text{PbTiO}_3$ .

### 2.5.1 Experimental

Figure 2.9 shows a picture of the MBE system. It is a modified VG MBE chamber. Titanium is evaporated from a Omicron Focus EFM 4 electron beam evaporation source. The flux was measured and controlled using the flux monitor of the evaporator. Lead oxide is evaporated from a Luxel Radak thermal evaporation cell. Atomic oxygen was supplied by a Oxford Scientific ECR plasma source fitted with a quartz delivery tube to ensure a high flux at the substrate surface. The substrates were mounted on stainless steel sample holders with spot-welded tantalum strips. The substrates were heated using a filament. Prior to the growth, the fluxes were calibrated using a quartz crystal monitor. The chamber is equipped with a Staib

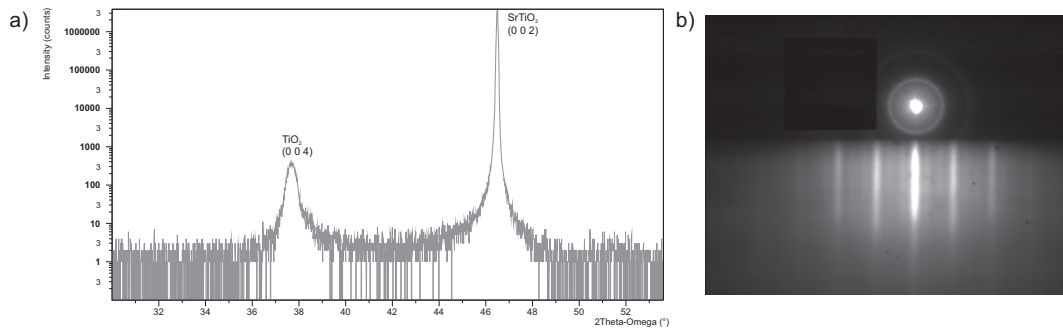


**Figure 2.10:** a) XRD pattern showing the  $\text{TiO}_2$  (anatase) (004) reflection and the (002)  $\text{SrTiO}_3$  substrate peak. b) RHEED pattern of a  $\text{TiO}_2$  thin film, showing satellite peaks close to the main spots that are typical for anatase [62]

electron gun and a phosphorous screen for RHEED. The electron energy used for RHEED was 15 keV. Various growth strategies were employed in this thesis for the growth of  $\text{PbTiO}_3$ . Some methods turned out to be more successful than others, but an overview of the results of the various growth approaches illustrates some of the chemistry and growth characteristics of the  $\text{PbTiO}_3$  system.

The most simple approach to MBE growth is coevaporation, where the lead(oxide), titanium and oxygen beams arrive simultaneously at the substrate surface. This method turns out to be not particularly successful. At a growth temperature of  $\approx 600^\circ\text{C}$  this method resulted in  $\text{TiO}_2$  films, showing peaks in XRD that seem to correspond to an anatase structure. This structure also shows a typical reconstruction in the RHEED pattern, see figure 2.10. [62] Films grown under these conditions show no sign of lead incorporation into the film. All the lead arriving at the surface re-evaporates into vacuum, despite the significant excess of lead that was used.

If coevaporation is used for growth at lower temperatures, between  $400^\circ\text{C}$  and  $500^\circ\text{C}$ , formation of  $\text{PbO}$  islands occurs. These  $\text{PbO}$  islands are easily recognized in RHEED by their 3D transmission pattern as shown in figure 2.6. The fact that  $\text{PbO}$  islands can form indicates that there is an excess of lead. Exact matching of the lead(oxide) and titanium fluxes turned out to be very difficult. If no excess of lead is supplied, the RHEED pattern quickly disappears, as no crystalline phase is formed.

Although using lead oxide ( $\text{PbO}$ ) instead of metallic lead, as a source material

does raise the evaporation temperature, and thus also the re-evaporation temperature slightly, no significant difference is observed in case of coevaporation. For the rest of the growth experiments  $\text{PbO}$  was used as a source material. The use of  $\text{PbO}$  also removes the kinetic and thermodynamic barriers for the oxidation of metallic lead and thus should be beneficial for  $\text{PbTiO}_3$  growth.

The proper stoichiometry arriving at the sample surface can also be obtained by using timing to control the number of particles arriving at the surface during every cycle. In general, the behavior of the growing films is similar to the previous case in that a high temperature growth would lead to an anatase film, and a low temperature growth with  $\text{PbO}$  excess would lead to  $\text{PbO}$  islands. When the timing was adjusted to obtain stoichiometry at relatively low growth temperatures ( $450^\circ\text{C}$ ), crystalline  $\text{PbTiO}_3$  films were obtained in some experiments. Other experiments resulted in amorphous films. However, ex-situ annealing of these films at a temperature of  $600^\circ\text{C}$  resulted in (001) oriented  $\text{PbTiO}_3$  films. Reproducibility is therefore the main issue when growing  $\text{PbTiO}_3$  by depositing the  $\text{PbO}$  and  $\text{TiO}_2$  sublayers separately. It seems that crystalline growth occurs from special sites such as steps and defects. When the number of special sites is too low, amorphous growth takes place rather than crystalline growth. This suggests that a higher growth temperature is required to reproducibly grow crystalline  $\text{PbTiO}_3$  films, but increasing the growth temperature in sublayer growth led to  $\text{TiO}_2$  films.

A way to enhance reproducibility is to use adsorption-controlled growth, in which the incorporation of lead is limited by the deposition of titanium. adsorption control was originally devised for MBE growth of  $\text{GaAs}$ . [86] For the growth of  $\text{PbTiO}_3$ , this method has been reported by Theis and Schlom, [60, 87] and recently, this method was also used for growing  $\text{BiFeO}_3$ . [88]

The advantage of adsorption-controlled growth is that the stoichiometry is very well controlled. The conditions must be such that lead in the  $\text{PbTiO}_3$  structure is stable and any excess of lead will re-evaporate into the vacuum. Experiments using different shuttering schemes already showed that at too low temperatures,  $\text{PbO}$  adsorption is not limited by  $\text{TiO}_2$  and a rough  $\text{PbO}$  rich film is formed. At too high temperatures, on the other hand,  $\text{PbO}$  does not stick to the surface at all, and  $\text{TiO}_2$

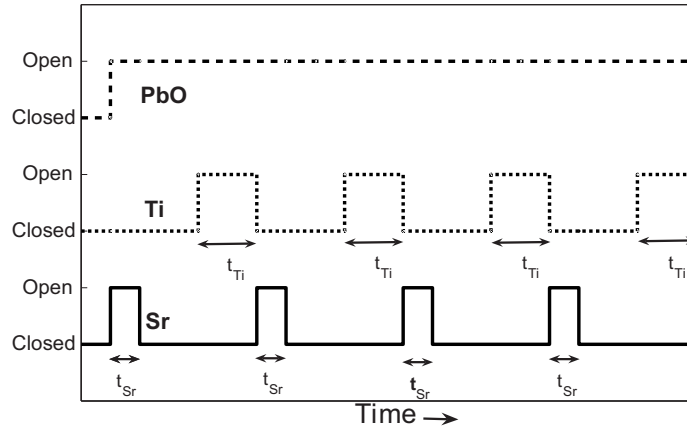


**Figure 2.11:** Shuttering scheme used for  $\text{Pb}_x\text{Sr}_{1-x}\text{TiO}_3$  growth. The titanium time corresponds to a single monolayer. The Strontium time determines the level of substitution.

films are grown. This is also found to be true as a function of the PbO flux, which can be taken as a PbO pressure over the substrate under the thermal conditions during growth. At a too low PbO flux, the PbO in the  $\text{PbTiO}_3$  is not stable and evaporates into vacuum. To prevent the re-evaporation of PbO, a constant flux of PbO is supplied to the substrate. From the coevaporation experiments it was found that even though an excess of Pb(O) is supplied, anatase layers are formed, suggesting that the interaction between the  $\text{TiO}_2$  layers is stronger than that between  $\text{TiO}_2$  and PbO layers. To ensure that PbO can form a full layer, Ti is supplied in monolayer doses. Between the Ti doses, PbO has time for form a full layer. A scheme of the shuttering during adsorption controlled growth is shown in figure 2.11.

Table 2.2 shows typical experimental parameters for the MBE growth of  $\text{Pb}_x\text{Sr}_{1-x}\text{TiO}_3$  thin films. Using these parameters, high quality thin films can be grown reproducibly. The shuttering scheme shown in figure 2.11 is employed. Varying the level of strontium substitution can be obtained by changing the strontium time ( $t_{\text{Sr}}$ ) at a fixed Sr flux. The  $\text{Pb}_x\text{Sr}_{1-x}\text{TiO}_3$  thin films in the remainder of this thesis have all been grown using this adsorption-controlled growth technique.

Current (A)	Pyrometer (°C)	Thermocouple 1 (°C)	Thermocouple 2 (°C)
3.6	640	667	648

a) Substrate heater parameters

Beam	Flux (Å/min)	Temperature (°)	E-beam power (W)	Time (s)
PbO	6.5	600		38*
Sr	3.0	500		0-24
Ti	1.5		24	42

b) Evaporation cell parameters

Gas	base pressure (mbar)	growth pressure (mbar)	Plasma source power (mA)
Oxygen	$2 \times 10^{-9}$	$5 \times 10^{-6}$	20

c) Oxidizing gas parameters

**Table 2.2:** Typical parameters as used in the growth of Pb<sub>x</sub>Sr<sub>1-x</sub>TiO<sub>3</sub> thin films. a) Substrate heater current and temperatures as measured using an optical pyrometer set to an emissivity of 0.7 and two different thermocouples close to the substrate. b) Fluxes and temperatures for the evaporation sources. (\*)The PbO shutter is open continuously, the time given is the time the Ti shutter is closed every cycle. c) Gas conditions.

### 2.5.2 Thermodynamic model of adsorption controlled growth

The stoichiometry control offered by the adsorption-controlled growth mechanism is one of the key features of the MBE growth of PbTiO<sub>3</sub>. In this section, a simple thermodynamic model of this growth mode will be presented.

Although thin film growth consists of a complex combination of thermodynamics and kinetics (section 2.2.2), pure thermodynamics can show how adsorption-controlled growth works. For this model, the molecular beams arriving at the surface are assumed to behave as a gas with a certain pressure. This pressure is related to the flux of the molecular beam ( $\Phi$  in  $\frac{\text{molecules}}{\text{m}^2\text{s}}$ ), the mass of the particles ( $m$  in kg) and the source temperature (K). This beam equivalent pressure is given by [87]

$$p = \frac{\Phi}{\cos\Theta} \sqrt{\frac{\pi m k_B T}{8}} \quad (2.5)$$

where  $p$  is the beam equivalent pressure (in Pa),  $\Theta$  is the incident angle of the molecular beam and  $k_B$  is the Boltzmann constant.

In this model, two processes are considered: The sublimation of PbO and the formation of PbTiO<sub>3</sub> from TiO<sub>2</sub> and PbO.

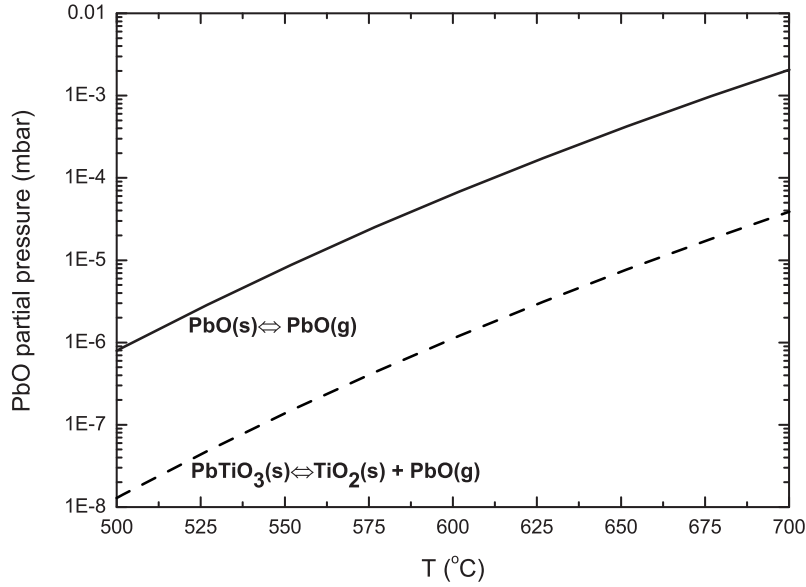
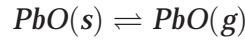


**Figure 2.12:** Phase diagram of  $\text{PbTiO}_3$  as a function on  $\text{PbO}$  partial pressure and temperature. After Theis et al. [87]



The interpretation of the first process is the condensation of a layer of  $\text{PbO}$  on a  $\text{PbO}$  terminated surface, which is equivalent to condensation on a bulk  $\text{PbO}$  crystal. The second process describes the condensation of  $\text{PbO}$  on a  $\text{TiO}_2$  terminated surface, creating a  $\text{PbTiO}_3$  unit cell. The equilibrium vapor pressures of  $\text{PbO}$  for both processes were calculated using the Gibbs energy of both processes.

$$\mu_{\text{PbO}(s)}(T) - \mu_{\text{PbO}(g)}(T) \ln\left(\frac{p}{p_0}\right) > 0 \quad (2.6)$$

$$\mu_{\text{PbTiO}_3(s)}(T) - \mu_{\text{TiO}_2(s)}(T) - \mu_{\text{PbO}(g)}(T) \ln\left(\frac{p}{p_0}\right) > 0 \quad (2.7)$$

where  $\mu_i(T)$  are the chemical potentials of species  $i$  at a temperature  $T$ , and  $p$  and  $p_0$  are the partial pressure and the reference pressure, respectively. Figure 2.12 shows the equilibrium vapor pressures as a function of temperature. Thermodynamic data was obtained from Barin. [89] From figure 2.12 it can be seen that there is a range, where  $\text{PbO}$  does evaporate from a  $\text{PbO}$  layer but not from a  $\text{TiO}_2$  layer.



When  $\text{PbTiO}_3$  is grown under these conditions, the  $\text{PbO}$  deposition is self-limiting; as long as the first  $\text{PbO}$  layer on top of a  $\text{TiO}_2$  layer is not filled, the arriving  $\text{PbO}$  molecules are in equilibrium with a  $\text{PbTiO}_3$  structure and will be incorporated into the film. However, if the  $\text{PbO}$  layer is complete, the gaseous  $\text{PbO}$  molecules are in equilibrium with the solid  $\text{PbO}$  surface, and no excess  $\text{PbO}$  will be deposited. During growth a constant supply of  $\text{PbO}$  has to be provided because if gaseous  $\text{PbO}$  is removed, the equilibrium will shift to the right and  $\text{PbTiO}_3$  will lose  $\text{Pb(O)}$ .

The flux of  $\text{PbO}$  in  $\text{PbTiO}_3$  growth is  $6.5 \text{ \AA}/\text{min}$  (table 2.2). Using equation (2.5) a beam equivalent pressure of  $3.6 \times 10^{-6} \text{ mbar}$  is obtained. In figure 2.12 it can be seen that this pressure at the growth temperature of  $640^\circ\text{C}$  does indeed fall in the adsorption-controlled growth region.

In summary, the main features of adsorption-controlled growth, such as the self-limiting behavior and the need to supply a constant flux of  $\text{PbO}$ , can be described by a thermodynamic model. The experimental parameters and observation are also consistent with the model.



